Polysaccharide-based chiral stationary phases as halogen bond acceptors: A novel strategy for detection of stereoselective σ-hole bonds in solution

Paola Peluso, Victor Mamane, Roberto Dallocchio, Alessandro Dessì, Rosaria Villano, Daniele Sanna, Emmanuel Aubert, Patrick Pale, Sergio Cossu

Polysaccharide-based chiral stationary phases as halogen bond acceptors: a novel strategy for detection of stereoselective σ-hole bonds in solution

Paola Peluso,[1,*] Victor Mamane,[2,*] Roberto Dallocchio,[1] Alessandro Dessì,[1] Rosaria Villano,[1] Daniele Sanna,[1] Emmanuel Aubert,[3] Patrick Pale[2] and Sergio Cossu[4]

[1] Istituto di Chimica Biomolecolare ICB CNR – Sede secondaria di Sassari, Sassari, Italy

[2] Institut de Chimie de Strasbourg, UMR 7177, Equipe LASYROC, Strasbourg, France

[3] CRM2, UMR CNRS 7036, Université de Lorraine, Vandoeuvre-les-Nancy, France

[4] Dipartimento di Scienze Molecolari e Nanosistemi, Università Ca' Foscari di Venezia, Mestre Venezia, Italy

RUNNING TITLE: Polysaccharide-based polymers as halogen bond acceptors

* **Correspondence:** Dr. Paola Peluso, Istituto di Chimica Biomolecolare ICB CNR – Sede secondaria di Sassari, Traversa La Crucca 3, Regione Baldinca, I-07100 Li Punti - Sassari, Italy. **E-mail:** p.peluso@icb.cnr.it

* Additional corresponding author: Dr. Victor Mamane, **E-mail:** vmamane@unistra.fr

Abbreviations: ACMPC, amylose *tris*(5-chloro-2-methylphenylcarbamate); **ADMPC**, amylose *tris*(3,5-dimethylphenylcarbamate); **CCMPC**, cellulose *tris*(3-chloro-4-methylphenylcarbamate); **CDMPC**, cellulose *tris*(3,5-dimethylphenylcarbamate); **CSP**, chiral stationary phase; **ECD**, electronic circular dichroism; **EEC**, entropy-enthalpy compensation; **EEO**, enantiomer elution order; **EP**, electrostatic potential; **EPS**, electrostatic potential surface; **ESH**, explicit σ-hole; **HB**, hydrogen bond; **Hex**, *n*-hexane; **IPA**, isopropyl alcohol; **MD**, molecular dynamic; **MeOH**, methanol; **PO**, polar organic; **XB**, halogen bond; **XBA**, halogen bond acceptor; **XBD**, halogen bond donor; **XRD**, X-ray diffraction

Keywords: Atropisomers / Enantioseparation / Halogen bond / Molecular dynamic / Polysaccharide-based chiral stationary phases

Abstract

In the last years, halogen bonds (XBs) have been exploited in a variety of research areas both in the solid state and in solution. Nevertheless, several factors make formation and detection of XBs in solution challenging. In addition, to date few chiral molecules containing electrophilic halogens as recognition sites have been reported. Recently, we described the first series of XB-driven enantioseparations performed on cellulose *tris*(3,5-dimethylphenylcarbamate) (CDMPC) by HPLC. On this basis, herein the performances of amylose *tris*(3,5-dimethylphenylcarbamate) (ADMPC) as XB acceptor were also investigated and compared with respect to CDMPC. With the aim to explore the effect of polysaccharide backbone on the enantioseparations, the thermodynamic parameters governing the halogen-dependent enantioseparations on both CDMPC and ADMPC were determined by a study at variable temperature and compared. Molecular dynamic simulations were performed in parallel in order to model the halogen bond in polysaccharide-analyte complexes. Chiral halogenated 4,4'-bipyridines were used as test compounds (XB donors). On this basis, a practical method for detection of stereoselective XBs in solution was developed, which is based on the unprecedented use of HPLC as technical tool with polysaccharide-based polymers as molecular probes (XB acceptors). The analytical strategy showed higher sensitivity for the detection of weak XBs compared to some spectroscopic techniques currently used in this field.

1 Introduction

A halogen bond (XB) is described as a noncovalent interaction between a covalently-bonded halogen (donor), bearing a region with a positive electrostatic potential (EP) (σ-hole) on unpopulated σ* orbitals, and a negative site (acceptor) (Fig. 1A) [1].
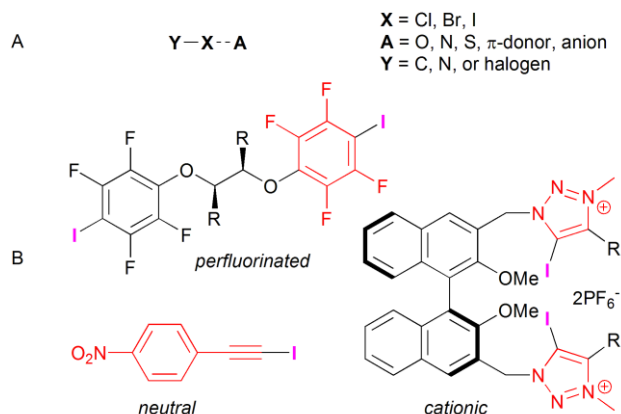
FIGURE 1 A: general description of XB; B: examples of perfluorinated, cationic, and neutral XBDs

This highly-directional attractive interaction, where halogens are involved not exclusively for their hydrophobic, inductive or steric effects [2], is characterized by R-X···acceptor angles close to 180°, and a strength increase for heavier halogens (Br, I). Indeed, the size of the σ-hole increases with the polarizability of the halogen following the order Cl < Br < I. Therefore, directionality and tunability are the key features which make XB a useful tool in crystal engineering and for the control of molecular assembly [3]. Although similar to the hydrophilic hydrogen bond (HB), the XB is hydrophobic, and this complementarity provides new opportunities for molecular recognition, particularly in solvated environment. Nevertheless, the exploration of solvent effects on XB has begun later compared to solid-state studies, and to date the applications in solution are still challenging [4]. Indeed, formation and detection of XBs in solution are more complicated compared to the solid state because the interactions can be influenced by conformational freedom of the molecules, a less ordered medium, and solvent effects on both donor and acceptor [5]. Another open issue concerns the application of XB in chiral systems, and few chiral molecules having σ-holes on halogens as recognition sites were described

recently [5-11]. Perfluorinated and cationic *N*-heterocyclic substructures (Fig. 1B) are able to activate

potential σ-hole sites and generate strong XBs, which are detectable by means of a variety of

spectroscopic techniques, NMR being the most widely used [12, see new ref]. On the other hand,

iodinated and brominated neutral XB donors (XBDs) lacking perfluorination are needed for real-life

applications in drug design [13] and supramolecular chemistry [14]. In general, in these cases,

spectroscopy weakly confirms the XB activity in solution. Therefore, in the last decade, the quest for

analytical methods characterized by higher sensitivity has been tackled [15].

Our groups have recently developed new procedures for the syntheses [16,17] and enantioseparations

[18] of halogenated chiral 4,4'-bipyridines which behaved as XBDs both in solution [19,20] and in the

solid state [17,21]. We discovered that XB-driven HPLC enantioseparations can be performed on

cellulose *tris*(3,5-dimethylphenylcarbamate) (CDMPC) as chiral stationary phase (CSP) [20].

Envisaging for polysaccharide derivatives a novel function other than resolution of racemic mixtures,

in this paper we show that HPLC coupled with polysaccharide-based CSPs as XB acceptors (XBAs)

can serve as analytical means for detection of weak stereoselective XBs in solution. Chiral halogenated

4,4'-bipyridines lacking perfluorination were used as XBD test compounds. The mechanistic bases of

this strategy were confirmed through a thermodynamic study performed at variable temperature as well

as enantiomer elution order (EEO) evaluation. Moreover, molecular dynamic (MD) simulations were

performed in order to model XB-based polysaccharide-analyte complexes.

2 Materials and methods

2.1 Instrumentation

An Agilent Technologies (Waldbronn, Germany) 1100 Series HPLC system [high-pressure binary

gradient system equipped with a diode-array detector operating at multiple wavelengths, a

programmable autosampler with a 20 μl loop and a thermostatted column compartment] was employed.

Data acquisition and analysis were carried out with Agilent Technologies ChemStation Version B.04.03

88   chromatographic data software. The UV absorbance is reported as milliabsorbance units (mAU). Lux

89   Cellulose-1 (cellulose *tris*(3,5-dimethylphenylcarbamate) (CDMPC)), Lux Cellulose-2 (cellulose *tris*(3-

90   chloro-4-methylphenylcarbamate)   (CCMPC)),   Lux   Amylose-1   (amylose   *tris*(3,5-

91   dimethylphenylcarbamate)   (ADMPC)),   Lux   Amylose-2   (amylose   *tris*(5-chloro-2-

92   methylphenylcarbamate) (ACMPC) (Phenomenex, USA), Chiralcel OD-H (CDMPC), and Chiralpak IA

93   (ADMPC) (Chiral Technologies Europe, France) were used as analytical (5 μm, 4.6 × 250 mm) chiral

94   columns. Dead time (t_0) was measured by injection of tri-*tert*-butylbenzene (Sigma-Aldrich, Germany)

95   as a non-retained compound [22]. Analyses were performed in isocratic mode. Chromatographic

96   separations were performed at 25°C. The flow rate (*FR*) was set at 0.8 ml/min for analytical separations.

97   The EEO was determined by injecting enantiomers of known absolute configuration (SI). The van't Hoff

98   experiments were conducted at 10, 15, 20, 25, 30 and 35 °C in a thermostatted column chamber

99   equipped with a cooling system. When the temperature was changed, the column was allowed to

100   equilibrate for 1 h before injecting the samples. Additional details on determination of thermodynamic

101   parameters are reported in SI.

102   **2.2 Chemicals and reagents**

103   *Rac*-**1**-**10** were synthesized as previously reported [16,17]. HPLC grade *n*-hexane (Hex), *n*-heptane,

104   methanol (MeOH) and 2-propanol (IPA) were purchased from Sigma-Aldrich (Taufkirchen, Germany).

105   **2.3 Computationals**

106   For 4,4'-bipyridines geometry optimization and computation of electrostatic potential surfaces (EPSs)

107   and related parameters (EP values are given in kJ/mol) were performed and graphically generated using

108   the Spartan'10 Version 1.1.0 [23] (Wavefunction Inc., Irvine, CA) program and employing the ab initio

109   DFT method with the B3LYP functional and the 6-311G* basis set (available for elements H-Ca, Ga-Kr

110   and I). The EP describes the value of the electrostatic potential onto an electron density surface and it

111   was used as an indicator of the charge distribution on the molecules. Min EP and max EP are the

112   minimum and the maximum values of the mapped property. EPS and molecular property calculations of

5

113 polysaccharide side chains and solvents were performed with the B3LYP functional and the 6-31G**

114 basis set. The carbamate frameworks were designed by substituting the glucosyl moiety with a methyl

115 group. All calculated EPS and experimental details for MD simulations are available in the SI.

3 Results and discussion

3.1 HPLC as technical tool

118 The strength of the XB is regulated by the depth of the σ-hole, the Lewis basicity of the XBA and the

119 stereoelectronic properties of the medium. Thus, with the aim to develop a sensitive analytical procedure

120 for detection and investigation of stereoselective XBs, HPLC on a chiral support acting as XBA was

121 envisaged as a versatile technical tool on the basis of the following remarks: *i*) detailed information on

122 primary and secondary stereoselective interactions between a chiral analyte, acting as potential XBD,

123 and a selector able to function as XBA could be derived from the chromatographic parameters [24,25];

124 *ii*) this technique works in a solvated medium, namely the mobile phase (MP), which can be easily

125 tuned, allowing solvent effects on both donor and acceptor to be studied; *iii*) the interaction is studied

126 under pressure (30-40 bar) inducing close contacts with an amplification of the contact extent compared

127 to techniques working at ambient pressure. In addition, several adsorption-desorption steps contribute to

128 the separation, increasing the sensitivity of the technique; *iv*) retention and separation are influenced by

129 temperature, so that thermodynamic parameters associated with halogen-dependent enantioseparation

130 could be determined by van't Hoff plots [26]; *v*) finally, the availability of the EEO is of high

131 importance in order to gain information on the topological approach toward the selector.

3.1.1 Polyhalogenated 4,4'-bipyridines as XBDs

133 4,4'-bipyridines **1**-**10** (Table 1) were used as neutral chiral non-perfluorinated XBD analytes. For all

134 halogenated substituents, the EPs were calculated in order to evaluate the σ-hole depth [20,27]. The

135 design was performed by means of halogen-driven structural and electronic engineering on the electron-

6

136   poor 4,4'-bipyridine core with the aim to obtain analytes whose chromatographic response was strictly

137   dependent on the σ-hole depth.

138   **TABLE 1** Calculated max EPs on the halogens (I, Br, Cl)

139

X = Cl (**1**)   X = Cl (**4**)   X = Cl (**6**)   X = Cl (**8**)   **10**
X = Br (**2**)   X = Br (**5**)   X = Br (**7**)   X = Br (**9**)
X = I (**3**)
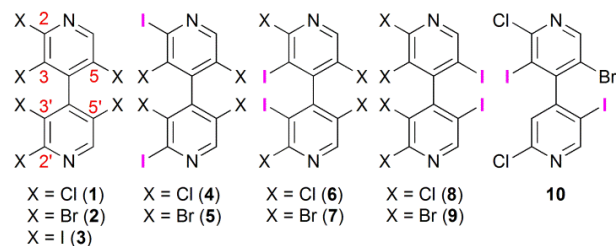
XBDs	max EP (kJ/mol)					
	X_{C2}	$X_{C2'}$	X_{C3}	$X_{C3'}$	X_{C5}	$X_{C5'}$
1	64.5	64.5	89.9	89.9	90.9	90.9
2	95.2	95.2	119.8	119.8	120.9	120.9
3	**120.5**	**120.5**	**144.2**	**144.2**	**146.8**	**146.8**
4	**127.4**	**127.4**	86.2	86.2	88.0	88.0
5	**123.1**	**123.1**	118.9	118.9	120.5	120.5
6	60.2	60.2	**154.3**	**154.3**	85.4	85.4
7	93.1	93.1	**148.0**	**148.0**	118.8	118.8
8	62.4	62.4	85.5	85.5	**154.4**	**154.4**
9	94.8	94.8	118.3	118.3	**149.3**	**149.3**
10	60.9	52.3	**151.3**	--	121.3	**144.1**

140
141   The comparison of the max EPs on iodine in compounds **6** and **11**-**14** (Fig. 2) evidenced the

142   combined electronic activation which is exerted on iodine σ-hole by the heterocyclic core and the

143   chlorine introduction at positions 2,2', **14** being a known perfluorinated XBD used as reference [28]. In

144   particular, compounds **1**-**3** were used in order to assess the behaviour of iodine, bromine and chlorine as

145   XBD sites. As in the solid state XBs can be assessed by the reduction of the sum of van der Waals radii

146   [29] between the interacting atoms *via* single crystal XRD, for **1**-**3** the extent of the penetration of the

147   van der Waals atomic spheres was shown to follow the reported XB strength (I > Br > Cl) (SI). On the

148   other hand, compounds **4**-**9** were selected as models focusing on the stereoelectronic environment of

iodine as privileged XBD site. In addition, **10** was specifically used in order to have two types of iodinated XBD sites in a single molecule, I_{C3} being (151.3 kJ/mol) more electronically activated and less sterically available than $I_{C5'}$ (144.1 kJ/mol). Indeed, as halogens are much larger and polarizable than hydrogen, XB is more sensitive to steric hindrance than HB [1].
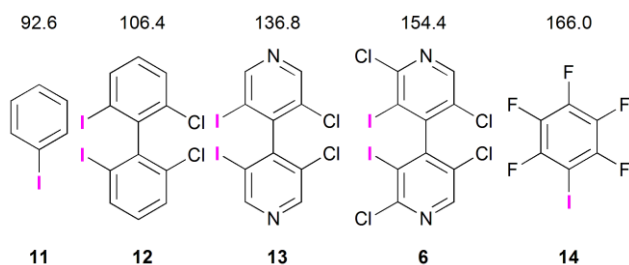
FIGURE 2 Comparison of calculated max EPs (kJ/mol) on iodine for **6** and **11**-**14** (Spartan'10 Version 1.1.0, DFT, B3LYP/6-311G*)

Therefore, in this context, halogen atoms serve as σ-hole donors, stereoelectronic modulators, and atropisomerism inductors by blocking 4,4'-axis rotation.

3.1.2 Polysaccharide dimethylphenylcarbamates as XBAs

We have recently demonstrated that XB-driven enantioseparations of halogenated 4,4'-bipyridines can be performed by HPLC on CDMPC [20], where XBs are formed between halogen substituents on the analyte and the carbonyl groups of the CSP. On this basis, we envisaged the possibility to use both cellulose- and amylose-based polymers as chiral probes for detection and systematic study of XBs (Table 2). In these CSPs, conformational chirality depends on the helical twist generated by the specific glycosidic 1,4 linkages in the cellulose (β) and amylose (α) chains [30]. Consequently, a chiral supramolecular environment surrounds the carbonyl XBA sites located in the inner polar layer, whereas an outer layer containing substituted aromatic rings is able to exert π–π, π-X and hydrophobic interactions [24,25]. On this basis, CDMPC and ADMPC were chosen as privileged probes which contain carbonyl oxygens with good properties as XBAs (min EP_{CO} = -170 kJ/mol). On the other hand, CCMPC and ACMPC were considered as terms of comparison. Indeed, for analytes able to exert XBs on CDMPC or ADMPC, lower separation factors were expected on CCMPC and ACMPC as results of

171 the reduced XBA capability of the carbonyls induced by the electron-withdrawing chloro-substituent

172 [31].

173 **TABLE 2** Structures of polysaccharides used as XBAs
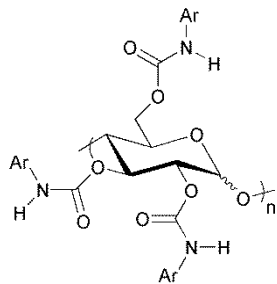
174

CSP	Ar- = (R,R')C₆H₃-	linkage	min EP$_{CO}$[a]
CDMPC	(3,5-dimethyl)	β-D	-169.98
ADMPC	(3,5-dimethyl)	α-D	-169.98
CCMPC	(3-chloro-4-methyl)	β-D	-155.82
ACMPC	(5-chloro-2-methyl)	α-D	-158.77

175 [a][kJ/mol]

176
177 3.1.3 The mobile phase as XB medium: solvent effect

178 Solvent effect could be evaluated by means of HPLC. On CDMPC the mixture Hex/IPA 90:10 (*mix*

179 *A*) had proved to assist XBs and, consequently, to produce high/moderate α values for compound with

180 good properties as XBDs. On the contrary, by enhancing MP polarity through addition of methanol

181 (MeOH) (Hex/IPA/MeOH 90:5:5) (*mix B*), selectivity decreased. Indeed, MeOH is able to destabilize

182 XBs [4] by penetrating inside the chiral cavity and forming HBs with the carbonyl oxygens better than

183 IPA due to its stereoelectronic properties (SI). Meanwhile, MeOH favours hydrophobic contacts [20].

184 3.2 HPLC XB-driven enantioseparations: CDMPC *vs* ADMPC

185 Six chromatographic systems generated by the combination of CDMPC, ADMPC, ACMPC with *mix*

186 *A;* and CDMPC and ADMPC with *mix B* as MPs were evaluated toward compounds **1**-**10** (SI). The

187 obtained α values are comparatively summarized in Fig. 3. Moreover, as both retention and separation

188 are influenced by temperature, a variable temperature study was carried out between 10 and 35 °C for all

189   bipyridines on the five chromatographic systems. Because the van't Hoff plots were linear in the

190   considered temperature range ($r^2 \geq 0.9900$), enthalpy and entropy values derived from the plots allowed

191   to evaluate the enthalpic and entropic contribution to halogen-dependent enantioseparations.
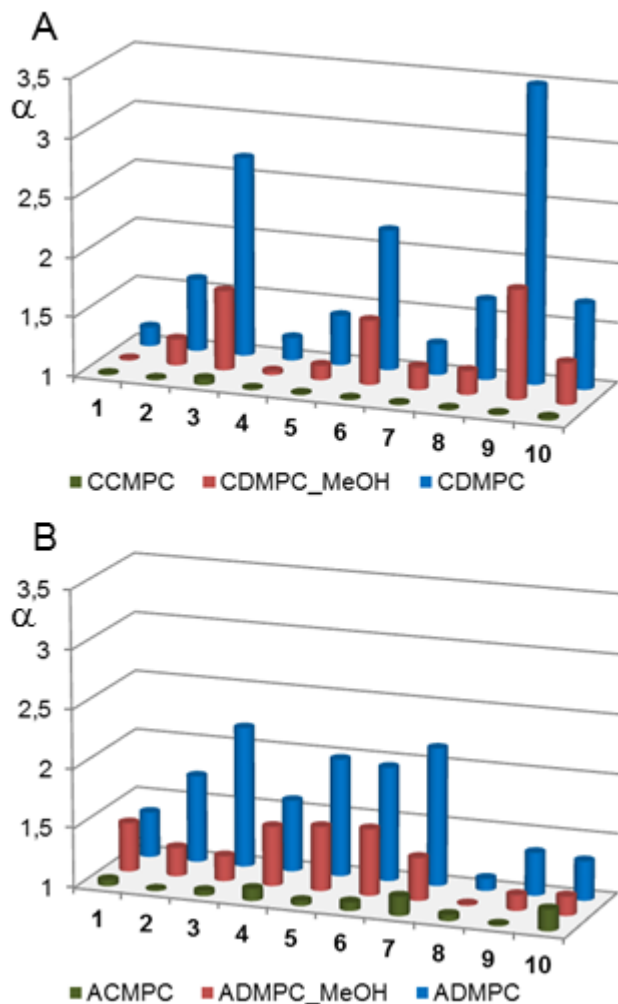
192

193   **FIGURE 3** Comparative outcomes of the XBD screening on cellulose- (A) and amylose-based (B) CSPs

194   On both CDMPC and ADMPC with *mix A*, retention and selectivity for compounds **1**-**3** increased

195   following the order Cl < Br < I ($0.44 \leq k_1 \leq 8.00$; $1.16 \leq \alpha \leq 2.68$), with *M-P* EEO in each case. In

196   accord with our initial hypotheses, evaluation of the chromatographic parameters obtained on both

197   CCMPC and ACMPC showed a dramatic decrease of selectivity values ($1.00 \leq \alpha \leq 1.05$).

198   Interestingly, on ADMPC selectivity increased compared to CDMPC for **1** (+19%) and **2** (+7.4%),

199   whereas it decreased for **3** (-18.6%). This behaviour could be explained taking into account that for

CDMPC the cavities are slightly bigger than for ADMPC which presents stronger intramolecular HBs [33]. Consequently, ADMPC cavity was more accessible for **1** (ESP volume 277.08 Å^3) and **2** (310.97 Å^3) and less available for **3** (373.43 Å^3). Therefore, a mixed enantioseparation mechanism controlled by halogen-dependent interactions as well as analyte steric fit seemed to be active on the amylose-based CSP, with chromatographic outcomes depending on both volume and XBD ability of the analyte. Differently, on CDMPC the σ-hole on halogens were shown to control enantioseparation exclusively [20]. The occurrence of two different mechanisms as the polysaccharide backbone changes was supported by the following remarks: *i*) $\Delta\Delta S$ values determined for **1**-**3** on CDMPC (-5.36 (**1**) > -19.78 (**2**) > -27.47 (**3**)) ranged following an opposite order compared to ADMPC (-5.95 (**1**) < -2.38 (**2**) < -0.55 (**3**)); *ii*) by enhancing MP polarity with *mix B* on CDMPC retention increased ($0.51 \leq k_1 \leq 8.11$), whereas selectivity decreased ($1.00 \leq \alpha \leq 1.67$), keeping again the order Cl < Br < I. Indeed, a percent increase of k_1 following the order Cl (15.9%) > Br (10.6%) > I (1.4%) could be observed, reasonably due to more favorable conditions for hydrophobic or steric fit driven retention mechanisms. On the contrary, retention of the second eluted enantiomer (*P*) (k2) showed a percent decrease following the order Cl (0%) < Br (-14.50%) < I (-36.7%), corresponding to the strength trend of XB interactions [1]. Differently, on ADMPC with *mix B*, retention of both enantiomers decreased with a percent decrease of k_1 following the order Cl (-31.9%) > Br (-12.6%) > I (-11.0%) and, conversely, following the order I (-50.3%) > Br (-37.5%) > Cl (-30.8%) for k_2. As a result, on ADMPC selectivity increased with *mix B* compared to *mix A* for **1** (+2.2%), whereas it decreased for **2** (-28.3%) and **3** (-44.5%); *iii*) for CDMPC the enthalpy-entropy compensation (EEC) straight line (r^2 = 0.9941) showed that the enantiodiscrimination mechanism (XB-driven) does not change over the analyte series (Fig. 4A). On the contrary, on ADMPC a deviation from linearity (r^2 = 0.7850) was observed in the EEC line, which confirmed the presence of other entropy-driven forces along with the XB (Fig. 4B); *iv*) on CDMPC, $\Delta\Delta H$ and $\Delta\Delta S$ values range from -0.79 to -14.23 kJ/mol and from -0.71 to -27.47 J/(mol K), respectively,

224 whereas on the ADMPC, higher $\Delta\Delta H$ (from -0.46 to -4.47 kJ/mol) and $\Delta\Delta S$ (from 0.31 to -11.07 J/(mol

225 K)) values were in a shorter range[VM1];
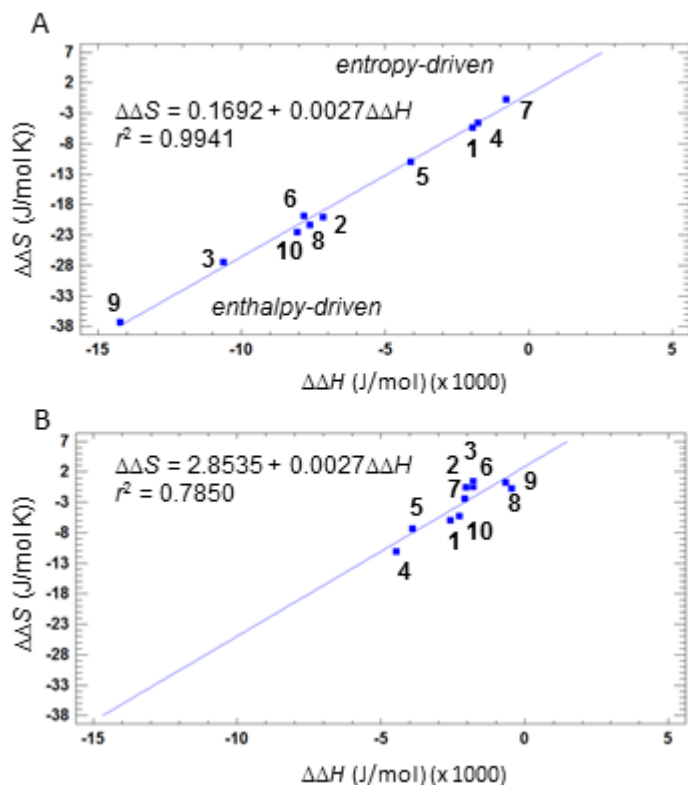
227 **FIGURE 4** EEC lines for 4,4'-bipyridines **1**-**10** on CDMPC (A) and ADMPC (B)

228   *v*) for compounds **4**-**10** selectivity decreased by using *mix B* on both CDMPC and ADMPC.

229 Nevertheless, only on CDMPC, both $\Delta\Delta H$ and $\Delta\Delta S$ values increased ranging from 0.06 to -7.59 kJ/mol

230 and from 0.48 to -20.08 J/(mol K), respectively. On the contrary, on ADMPC, $\Delta\Delta H$ and $\Delta\Delta S$ tended to

231 decrease, with values ranging from -0.45 to -8.74 kJ/mol and from 1.31 to -17.55 J/(mol K),

232 respectively; *vi*) on CDMPC, the topological approach to the polymeric XBA was iodine-dependent.

233 Indeed, iodine at positions 5,5' (**8** and **9**) induces a preference for *M-P* as EEO, whereas iodine at

234 positions 3,3' (**6** and **7**) induces the reverse EEO, *P-M*. As **10** also showed *P-M* as EEO, we assumed the

235 pivotal role of the 3-iodine in this case, although the medium extent of separation[VM2][PP3][VM4] (α: 1.67 (**8**) < 1.72

236 (**10**) < 2.18 (**6**)) suggested a cooperative effect of the two kind of iodines. On ADMPC the EEO was *M-*

237 *P* in almost all cases, confirming that the approach of the analytes tended to depend on their shape (steric

12

238   fit). In this regard, it is interesting to note that on ADMPC, MeOH-induced inversion of the elution order

239   (*P-M*) could be observed for **3** and **9** compared to *mix A* (*M-P*). Differently, by using *mix A*, backbone-

240   induced inversion of EEO could be observed for **6** and **7** on ADMPC (*M-P*) with respect to CDMPC (*P-*

241   *M*).

242   The comparative evaluation of the chromatographic parameters of tetrachlorinated **4**, **6**, and **8**

243   obtained with the system CDMPC-*mix A* highlighted the pivotal role of iodine as XBD site able to exert

244   stereoselective interactions. Indeed, α of **6** and **8**, bearing iodines close to the chiral axis, are higher

245   (+83.6% and +40.3%, respectively) than the corresponding value of **4**, whose 2,2'-iodines are located far

246   from the chiral axis. Analogously to that observed for **4** and **8**, α value ~~derived~~[VMS] obtained for the

247   2,2',3,3'-tetrabromo-5,5'-diiodo **9** is higher (+146%) than the corresponding value of the 2,2'-diiodo **5**.

248   Differently, for the 3,3'-diiodo **7** α decreased compared to **5**. In this case, the comparison of the $\Delta\Delta S$

249   values derived from the van't Hoff plots and associated with the enantiodiscriminations ([J/(mol·K], **5**: -

250   10.92; **7**: -0.71) proved that entropic factors, caused by the larger 2,2'-bromines close to the 3,3'-iodines,

251   exert a detrimental effect on selectivity [20]. Differently, on ADMPC-*mix A*, iodine at position 5,5'

252   seemed to be detrimental for enantioseparation. Indeed, **8**, **9** and **10** showed lower values of selectivity

253   ($1.10 \leq \alpha \leq 1.36$) compared to compounds bearing iodine in positions 3,3' and 2,2' ($1.60 \leq \alpha \leq 2.16$).

254   **3.3 Molecular dynamics of 6 and 8 on CDMPC and ADMPC**

255   MD calculations (see SI for details) were performed to simulate the interaction modes of the 4,4'-

256   bipyridines **6** and **8** with CDMPC and ADMPC. In this study, molecular models of 9-mer CDMPC and

257   ADMPC were constructed in order to confirm the halogenated binding sites for the enantiomers of **6** and

258   **8**. On the basis of our previous work in the field [20], the extra point [34], or explicit σ-hole (ESH) [35]

259   concept was used to model the XB in polysaccharide-haloanalytes complexes. Moreover, with the aim to

260   compare qualitatively the MD outcomes associated with different molecular situations, the calculations

261   were performed with and without the ESH, and Hex and MeOH solvent effects were taken into account

262 in accord with the methods used in the HPLC screening. Table 3 shows the values associated with I-

263 driven contacts found in the MD runs over 10 ns (ESH, solvent box, *n*-hexane).

264 **TABLE 3** Calculated geometrical parameters of (I···O) polysaccharide-analyte interactions[a]

polysaccharide	XBD	HPLC[b]		MD			
		t_R	obs.	CDMPC-enantiomer complex	$d_{I···O}$ (Å)[c,d]	C-I···O angle (°)	I···O=C angle (°)
CDMPC	**6**	8.27	(*P*)	(*P*)	3.41 (-2.6)	146.86	121.22
		13.83	(*M*)	(*M*)	3.08 (-12.0)	166.70	125.15
					3.14 (-10.3)	170.38	125.56
	8	7.98	(*M*)	(*M*)	3.00 (-14.3)	171.25	162.10
		10.95	(*P*)	(*P*)	3.26 (-6.9)	174.25	127.19
					3.60 (π···I)		
ADMPC	**6**	9.10	(*M*)	(*M*)	3.70 (π···I)		
		14.46	(*P*)	(*P*)	3.17 (-9.4)	169.42	135.03
					3.40 (-2.8)	160.39	122.95
	8	7.06	(*M*)	(*M*)	3.30 (π···I)		
		7.43	(*P*)	(*P*)	3.14 (-10.3)	169.15	159.57
					3.30 (-5.7)	164.79	123.50

265 [a]MD conditions: ESH; solvent box, *n*-hexane.
266 [b]Lux Cellulose-1 (CDMPC) or Lux Amylose-1 (ADMPC), Hex/IPA 90:10 v/v, *FR* 0.8 ml/min, t_R [min].
267 [c]ΣrvdW (I,O) = 3.5 Å [28].
268 [d]Penetration parameters I···O% = $100 \times \{(d_{I···O})/(r_{vdWI} + r_{vdWO}) - 1)\}$, where $d_{I···O}$ is the interatomic distance and rvdW the corresponding
269 van der Waals radii, are reported in brackets.
270

271 The iodinated analogues **6** and **8** showed distribution of I···O distances clustering around 3.00-3.41 Å

272 with penetration parameters ranging from -2.6% to -14.3% (sum of the van der Waals radii for I,O = 3.5

273 Å) [24]. Moreover, the C—I···O angles ranged from 160.39° to 174.25° in almost all cases and only for

274 the complex CDMPC-(*P*)-**6** a lower value of 146.86° was observed. In general, angles ranging from

275 160° to 180° are considered acceptable to decide if the interaction corresponds to a halogen bond [20].

276 Analogously, the X···O—C angles showed a distribution ranging from 121.22° to 135.03° and only for

277 the complexes of (*M*)- and (*P*)-**8** on CDMPC (162.10°) and ADMPC (159.57°), respectively, a deviation

278 from the reference value of 120° was observed. All[PP6][VM7] these observations (penetration of van der

279 Waals spheres and interaction angles) can be considered as an evidence of the implication of XB. [VM8]It

280 is worth mentioning that in all cases two I-driven interactions are observed for the second eluted

281 enantiomers compared to the single I-driven interaction observed for each first eluted enantiomers. As

282 consequence, the MD outcomes was showed to be in accord with the experimental EEO. As expected,

283   no I···O interactions were observed when ESH correction was not applied or when MeOH was

284   introduced in the solvent box instead of Hex.

285   In addition, with the aim to explore the recognition sites on both donor-analyte and acceptor-

286   polysaccharide, the potential contacts occurring in the course of the molecular dynamics were examined.

287   Indeed, taking into account the dynamic feature of the enantioseparation event, we analysed statistically

288   the distances between each of the six halogen (2 iodines, 4 chlorines) on 4,4'-bipyridine **6** (as donor

289   recognition sites) and fourteen points (N, O, H) located on each monomers of the CDMPC and ADMPC

290   nonamers (Fig. 5).
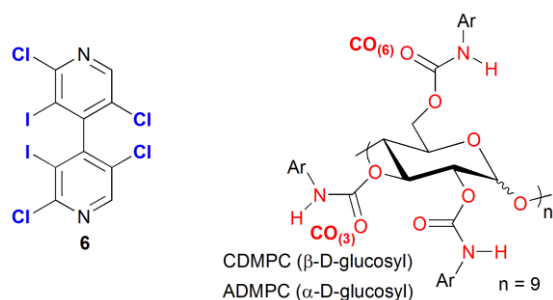
291

292   **FIGURE 5** Schematic representations of the contact sites analysed on **6**, CDMPC, and ADMPC in the course of MD

293   simulations

294   The contact distances were acquired (5000 steps) during the molecular dynamic time (10 ns). All

295   collected values within 6 Å were extracted (see SI for details) in order to evaluate the sites involved in

296   close contacts, without considering the type of interactions. From the calculated distribution values

297   associated with the selected recognition sites (Fig. 6), we observed that the (*P*) and (*M*) atropisomers

298   which are the first eluted enantiomers on CDMPC and ADMPC, respectively, presented the 3-iodine as

299   privileged recognition site (53.8% and 59.3%) and the carbonyl of the carbamate framework at C_6 as the

300   most frequent recognition sites (29.8% and 34.8%). Differently, on CDMPC the atropisomer (*M*) as

301   second eluted enantiomers showed two iodines as privileged sites with a distribution of 62.1%.

302   Analogously, for the second eluted atropisomer (*P*) on ADMPC the two iodine at 3,3'-positions

303   interacted with the polysaccharide with a distribution value of 80.7%. For both second eluted

15

304   enantiomers, the privileged recognition site is the carbonyl framework at C_3 (29.2% and 52.9% on

305   CDMPC and ADMPC, respectively).
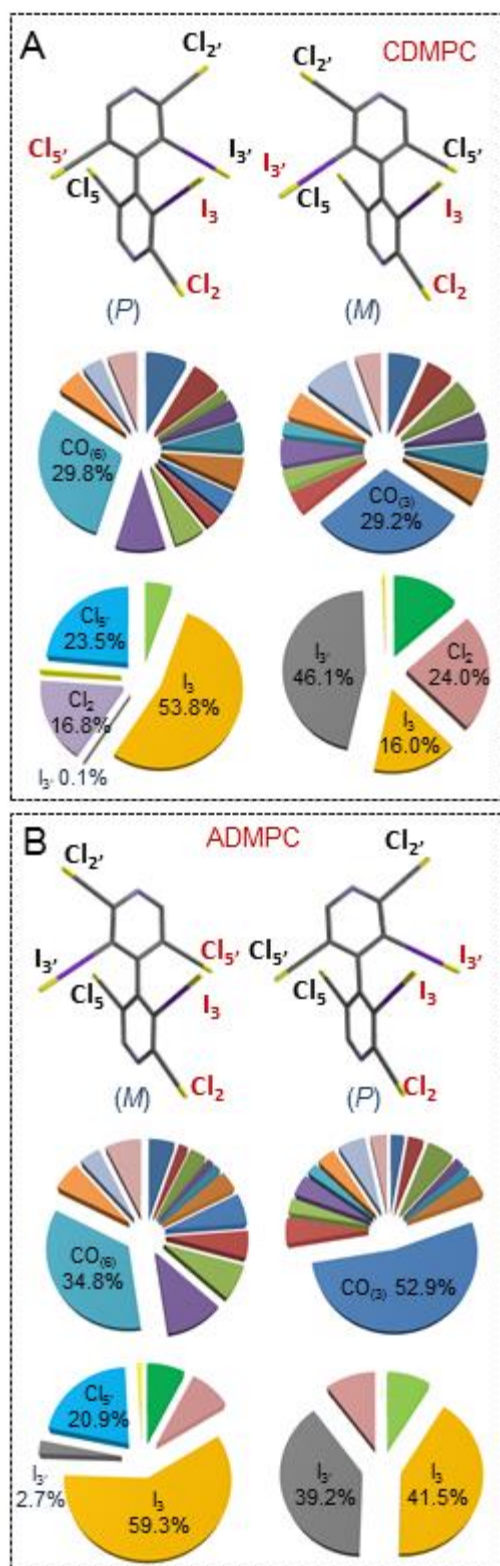
306
307   **FIGURE 6** Distribution of the interaction sites in the course of MD simulations (10 ns) of **6** enantiomers on 9-mers of both
308   CDMPC and ADMPC

309   Again, the results of the statistical evaluation of the observed contacts in the course of the four MDs

310   appeared consistent with the experimental EEOs.

311   **3.4 A novel strategy for detection of stereoselective σ-hole bonds in solution**

312   By the chromatographic, thermodynamic and computational evaluation, a protocol based on a three-

313   step orthogonal on-column screening has been set up to probe and detect XBs. Cellulose-based CSPs

314   appeared suitable for the purpose furnishing for **1**-**10**, used as XBD probes, chromatographic responses

315   strictly dependent on the occurrence of XBs, σ-hole depth and iodine regiochemistry. In Table 4, the

316   expected behaviours, as XBA, XBD and MP change, are summarized. Nevertheless, also amylose-based

317   CSPs proved to be useful in this field allowing to assess steric effects on XBs.

318   **TABLE 4** HPLC protocol to detect XB interactions
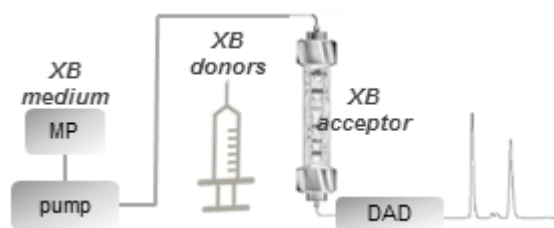
319

XBD	mechanism	CSP[a]	MP[b]	α[c] range
good	XB-driven	CDMPC	A	1.26-3.50
good	hydrophobic	CCMPC	A	1.00-1.05
good	XB-driven	CDMPC	B	1.00-1.92
poor	hydrophobic	CDMPC	A	< 1.2

320   [a]CDMPC cellulose *tris*(3,5-dimethylphenylcarbamate), CCMPC
321   cellulose *tris*(3-chloro-4-methylphenylcarbamate), ADMPC amylose
322   *tris*(3,5-dimethylphenylcarbamate), ACMPC amylose *tris*(5-chloro-2-
323   methylphenylcarbamate).
324   [b]Hex/IPA 90:10, *FR* = 0.8 ml/min (A), Hex/IPA/MeOH 90:5:5, *FR* =
325   0.8 ml/min (B); hex = *n*-hexane, IPA = 2-propanol, MeOH =
326   methanol.
327   [c]α separation factor.

328

329   Finally, as spectroscopic techniques have been widely used in this field [12], ESR and NMR

330   experiments were carried out (SI) to gain an insight into the sensitivity of the techniques toward some

331   4,4'-bipyridyl XBD probes. These experiments poorly confirmed the XBD activity proving the higher

332   sensitivity of HPLC for detection of weak stereoselective XBs in solution.

17

3.5 Halogen-dependent enantioseparations under aqueous-organic elution mode: a perspective

With the aim to explore the effect of water on halogen-dependent enantioseparations, the chromatographic behaviour of compounds **1**-**3** and **6** were investigated on ADMPC by using MeOH 100%, ACN 100%, MeOH/water 90:10, ACN/water 90:10 and ACN/water 80:20. The results of the screening are reported in Table 5.

TABLE 5 HPLC parameters (α, R_s) with PO and aqueous MPs[a]

XBD		MP				
		MeOH/water		ACN/water		
		10:0	9:1	10:0	9:1	8:2
1	α	**1.37**	1.00	1.06	1.05	1.04
	R_s	**2.4**	0.0	0.2	0.4	0.6
2	α	**1.52**	1.00	1.00	1.00	1.03
	R_s	**3.0**	0.0	0.0	0.0	0.4
3	α	1.00	1.00	**1.46**	**1.50**	**1.53**
	R_s	0.0	0.0	**3.7**	**6.3**	**6.7**
6	α	**2.27**	1.00	1.00	**1.12**	**1.13**
	R_s	**3.6**	0.0	0.0	**2.1**	**2.2**

[a]Column: Lux Amylose-1 (ADMPC), FR = 0.8 ml/min.

By using pure MeOH as MP, only compound **3** was completely unresolved indicating that ~~, thus~~ the steric fit ~~seemed to~~ ha~~s~~ve a pivotal effect on enantioseparation ~~extent. and The~~ Addition of water in the MP ~~proved to be~~ was detrimental for the enantioseparation of **1**, **2** and **6**[VM9]. ~~Also with the aqueous MP, the steric fit seemed to have a pivotal effect on enantioseparation extent~~[VM10]. On the contrary, by using pure ACN which favours polar interactions more than MeOH, ~~only~~ compound **3** was well enantioseparated and the gradual increase of water content in the MP had a beneficial effect only on ~~the~~ iodine-substituted compounds **3** and **6**[VM11]. These results evidenced the complementary behaviour of ACN compared to MeOH as MP in halogen-dependent enantioseparations, and an interesting effect of water in ~~the~~ iodine-dependent enantioseparations performed in aqueous ACN.

4 Concluding remarks

The on-column screening of halogenated 4,4'-bipyridines, used as test compounds, proved the efficacy and the potential of HPLC and cellulose-based polymers as technical and molecular tools, respectively, for the detection of stereoselective σ-hole bonds. On the other hand, on amylose-based

18

CSPs both chromatographic and thermodynamic results evidenced that other entropy-driven forces act along with halogen-dependent interactions allowing to study steric effects acting on halogen bonds in solution. Significantly, halogen-dependent enantioseparations have been observed on ADMPC by using water-containing MPs. This result allows to envisage the possibility to study water effects on σ-hole-driven interactions by HPLC. In this regard, it is worth mentioning that for medicinal chemistry applications, water is the exclusive solvent, and the behaviour of XB in water is still poorly understood.

5 References

1. Politzer, P., Murray, J. S., Clark, T., Halogen bonding and other σ-hole interactions: a perspective. *Phys. Chem. Chem. Phys.* 2013, *15*, 11178-11189.

2. Erdelyi, M., A big hello to halogen bonding. *Nature Chem.* 2014, *6*, 762-764.

3. Cavallo, G., Metrangolo, P., Milani, R., Pilati, T., Priimagi, A., Resnati, G., Terraneo, G., The halogen bond. *Chem. Rev.* 2016, *116*, 2478-2601.

4. Carlsson, A. -C. C., Veiga, A. X., Erdelyi, M., Halogen bonding in solution. *Top. Curr. Chem.* 2015, *359*, 49-76.

5. Kaasik, M., Kaabel, S., Kriis, K., Järving, I., Aav, R., Rissanen, K., Kanger, T., Synthesis and characterisation of chiral triazole-based halogen-bond donors: halogen bonds in the solid state and in solution. *Chem. Eur. J.* 2017, *23*, 7337-7344.

6. Lieffrig, J., Le Pennec, R., Jeannin, O., Auban-Senzier, P., Fourmigué, M., Toward chiral conductors: combining halogen bonding ability and chirality within a single tetrathiafulvalene molecule. *CrystEngComm* 2013, *15*, 4408-4412.

7. He, W., Ge, Y. -C., Tan, C. -H., Halogen-bonding-induced hydrogen transfer to C=N bond with Hantzsch ester. *Org. Lett.* 2014, *16*, 3244-3247.

8. Lieffrig, J., Niassy, A. G., Jeannin, O., Fourmigué, M., Halogen-bonded halide networks from chiral neutral spacers. *CrystEngComm* 2015, *17*, 50-57.

9. Nicolas, I., Jeannin, O., Pichon, D., Fourmigué, M., Dibromohydantoins as halogen bond (XB) donors: a route toward the introduction of chirality in halogen bonded systems. *CrystEngComm* 2016, *18*, 9325-9333.

10. Lim, J. Y. C., Marques, I., Ferreira, L., Félix, V., Beer, P. D., Enhancing the enantioselective recognition and sensing of chiral anions by halogen bonding. *Chem. Commun.* 2016, *52*, 5527-5530.

11. Lim, J. Y. C., Marques, I., Félix, V., Beer, P. D., Enantioselective anion recognition by chiral halogen-bonding [2]rotaxanes. *J. Am. Chem. Soc.* 2017, *139*, 12228-12239.

12. Erdelyi, M., Halogen bonding in solution. *Chem. Soc. Rev.* 2012, *41*, 3547-3557.
Ciancaleoni, G., Characterization of halogen bonded adducts in solution by advanced NMR techniques. Magnetochemistry 2017, 3, doi: 10.3390/magnetochemistry3040030

13. Wilcken, R., Liu, X., Zimmermann, M. O., Rutherford, T. J., Fersht, A. R., Joerger, A. C., Boeckler, F. M., Halogen-enriched fragment libraries as leads for drug rescue of mutant p53. *J. Am. Chem. Soc.* 2012, *134*, 6810-6818.

14. Dumele, O., Wu, X, Trapp, N., Goroff, N. S., Diederich, F., Halogen bonding of (iodoethynyl)benzene derivatives in solution. *Org. Lett.* 2014, *16*, 4722-4725.

15. Hakkert, S. B., Gräfenstein, J., Erdelyi, M., The ^{15}N NMR chemical shift in the characterization of weak halogen bonding in solution. *Faraday Discuss.* 2017, DOI: 10.1039/C7FD00107J.

16. Mamane, V., Aubert, E., Peluso, P., Cossu, S., Lithiation of prochiral 2,2'-dichloro-5,5'-dibromo-4,4'-bipyridine as a tool for the synthesis of chiral polyhalogenated 4,4'-bipyridines. *J. Org. Chem.* 2013, *78*, 7683-7689.

17. Mamane, V., Peluso, P., Aubert, E., Cossu, S., Pale, P., Chiral hexahalogenated 4,4'-bipyridines. *J. Org. Chem.* 2016, *81*, 4576-4587.

405   18.   Peluso, P., Mamane, V., Aubert, E., Cossu, S., High-performance liquid chromatography
406   enantioseparation of polyhalogenated 4,4'-bipyridines on polysaccharide-based chiral stationary
407   phases under multimodal elution. *J. Sep. Sci.* 2014, *37*, 2481-2489.

408   19.   Peluso, P., Mamane, V., Aubert, E., Cossu, S., Insights into the impact of shape and electronic
409   properties on the enantioseparation of polyhalogenated 4,4'-bipyridines on polysaccharide-type
410   selectors. Evidence of stereoselective halogen bonding interactions. *J. Chromatogr. A* 2014, *1345*,
411   182-192.

412   20.   Peluso, P., Mamane, V., Aubert, E., Dessì, A., Dallocchio, R., Dore, A., Pale, P., Cossu, S.,
413   Insights into halogen bond-driven enantioseparations. *J. Chromatogr. A* 2016, *1467*, 228-238.

414   21.   Abboud, M., Mamane, V., Aubert, E., Lecomte, C., Fort, Y., Synthesis of polyhalogenated 4,4'-
415   bipyridines via a simple dimerization procedure. *J. Org. Chem.* 2010, *75*, 3224-3231.

416   22.   Koller, H., Rimböck, K.-E., Mannschreck, A., High-pressure liquid chromatography on
417   triacetylcellulose : characterization of a sorbent for the separation of enantiomers. *J. Chromatogr.*
418   *A* 1983, *282*, 89-94.

419   23.   Shao, Y., Molnar, L. F., Jung, Y., Kussmann, J., Ochsenfeld, C., Brown, S. T., Gilbert, A. T. B.,
420   Slipchenko, L. V., Levchenko, S. V., O'Neil, D. P., Di Stasio Jr., R. A., Lochan, R. C., Wang, T.,
421   Beran, G. J. O., Besley, N. A., Herbert, J. M., Lin, C. Y., VanVoorhis, T., Chien, S. H., Sodt, A.,
422   Steele, R. P., Rassolov, V. A., Maslen, P. E., Korambath, P. P., Adamson, R. D., Austin, B.,
423   Baker, J., Byrd, E. F. C., Dachsel, H., Doerksen, R. J., Dreuw, A., Dunietz, B. D., Dutoi, A. D.,
424   Furlani, T. R., Gwaltney, S. R., Heyden, A., Hirata, S., Hsu, C. -P.; Kedziora, G., Khalliulin, R. Z.,
425   Klunzinger, P., Lee, A. M., Lee, M. S., Liang, W. Z., Lotan, I., Nair, N., Peters, B., Proynov, E. I.,
426   Pieniazek, P. A., Rhee, Y. M., Ritchie, J., Rosta, E., Sherrill, C. D., Simmonett, A. C., Subotnik, J.
427   E., Woodcock III, H. L., Zhang, W., Bell, A. T., Chakraborty, A. K., Chipman, D. M., Keil, F. J.,
428   Warshel, A., Hehre, W. J., Schaefer, H. F., Kong, J., Krylov, A. I., Gill, P. M. W., Head-Gordon,

M., Advances in methods and algorithms in a modern quantum chemistry program package. *Phys. Chem. Chem. Phys.* 2006, *8*, 3172-3191.

24. Lämmerhofer, M., Chiral recognition by enantioselective liquid chromatography: mechanisms and modern chiral stationary phases. *J. Chromatogr. A* 2010, *1217*, 814-856.

25. Scriba, G. K. E., Chiral recognition in separation science - an update. *J. Chromatogr. A* 2016, *1467*, 56-78.

26. O'Brien, T., Crocker, L., Thompson, R., Thompson, K., Toma, P. H., Conlon, D. A., Feibush, B., Moeder, C., Bicker, G., Grinberg, N., Mechanistic aspects of chiral discrimination on modified cellulose. *Anal. Chem.* 1997, *69*, 1999-2007.

27. Bondi, A., van der Waals Volumes and Radii. *J. Phys. Chem.* 1964, *68*, 441-451.

28. Aakeröy, C. B., Wijethunga, T. K., Desper, J., Đaković, M., Electrostatic potential differences and halogen-bond selectivity. *Cryst. Growth Des.* 2016, *16*, 2662-2670.

29. Präsang, C., Whitwood, A. C., Bruce, D. W., Halogen-bonded cocrystals of 4-(N,N-dimethylamino)pyridine with fluorinated iodobenzenes. *Cryst. Growth Des.* 2009, *9*, 5319-5326.

30. Chankvetadze, B., Recent developments on polysaccharide-based chiral stationary phases for liquid-phase separation of enantiomers. *J. Chromatogr. A* 2012, *1269*, 26-51.

31. Peluso, P., Mamane, V., Aubert, E., Cossu, S., High-performance liquid chromatography enantioseparation of atropisomeric 4,4'-bipyridines on polysaccharide-type chiral stationary phases: impact of substituents and electronic properties. *J. Chromatogr. A* 2012, *1251*, 91-100.

32. Yamamoto, C., Yashima, E., Okamoto, Y., Structural analysis of amylose tris(3,5-dimethylphenylcarbamate) by NMR relevant to its chiral recognition mechanism in HPLC. *J. Am. Chem. Soc.* 2002, *124*, 12583-12589.

33. Kasat, R. B., Wang, N. -H. L., Franses, E. I., Effects of backbone and side chain on the molecular environments of chiral cavities in polysaccharide-based biopolymers. *Biomacromol.* 2007, *8*, 1676-1685.

454   34.   Ibrahim, M. A. A., Molecular mechanical perspective on halogen bonding. *J. Mol. Model.* 2012,

455   *18*, 4625-4638.

456   35.   Kolář, M. H., Hobza, P., Bronowska, K., Plugging the explicit σ-holes in molecular docking.

457   *Chem. Commun.* 2013, *49*, 981-983.